Supplementary Material (ESI) for Chemical Communications

Carbohydrate assisted fluorescence *turn-on* gluco-imino-anthracenyl conjugate as Hg(II) sensor in milk and blood serum milieu

Atanu Mitra, Ankit Kumar Mittal and Chebrolu Pulla Rao[a,*]

SI 01: Synthesis and characterization of **L** & **C1**, **C2** and **C3**

Synthesis of **L**: To a suspension of glucosamine hydrochloride (2.15 g, 10 mmol) in ethanol (20 ml), triethlamine was added and stirred for 15 min and then 9-anthracenaldehyde (2.06 g, 10 mmol) was added. The reaction mixture was allowed to reflux at 70º C for 24 hrs during which a yellow solid was formed. The reaction mixture was cooled to RT and the product was separated by filtration and washed with a small portions of ethanol followed by ice cold $CHCl_3$ and then with diethylether followed by dried under vacuum. Yield (2.53 g, 69%); IR (KBr): 3412 (b) $\upsilon_{(O-H)}$, 2981(S) & 3296(S) $\upsilon_{(C-H)}$, 1615(S) $\delta_{(CH=N)}$, 1418 (S) and 1538 (S) $\delta_{(C=C)}$ cm^{-1}, ^1H NMR (DMSO-d_6):3.22-3.80 (m. 6H, C2-H, C3-H, C4-H, C5-H and C6-H), 4.60-5.12 (2d & 2t, 4O-H, C2-OH, C3-OH, C-4OH, C6-OH), 6.83-6.85 (d, H, $^3J_{C1-H-C2-H}$ 7.3 Hz, C1-H), 7.52-7.57 (m, 4H, Ar-C3Hs and Ar-C4Hs), 8.12-8.14 (m, 2H, Ar-C5Hs), 8.58-8.61 (m, 2H, Ar-C2Hs), 8.68 (s, 1H, Ar-C10H), 9.26(S, H, CH=N) ppm; ^{13}C NMR (DMSO-d_6): δ 95.66 (C1), 61.30-79.53 (C2-C6), 125.50-130.80 (Ar-10C), 161.51(CH=N) ppm; ESI MS: m/z 368 ($[M+H]^+$, 100%) Anal. calcd. for $C_{21}H_{21}O_5N$: C, 68.65; H, 5.76; N, 3.81 found C, 68.52; H, 5.77; N, 3.87.

Synthesis of **C1**: A 2.15 g of glucosylamine hydrochloride salt was suspended in ethanol. Etherial trietylamine solution was added dropwise to neutralize the acidic counterpart (pH = 7 - 8) and 2-hydroxy-1-naphthaldehyde (1.8 g, 10.5 mmol) was added to it. Bright yellow solid formed immediately. The mixture was refluxed for 6 h at ~60 ºC. The solid formed was filtered and washed with ice cold ethanol followed by diethyl ether. The compound was dried under vaccum and stored at 4 ºC. Yield (2.07 g, ~62 %) ^1H NMR (DMSO-d_6, ppm): δ 2.5 (q, 6H, DMSO-Hs), 3.12 - 3.75 (m, 5H, C2-H, C3-H, C4-H, C5-H & C6-H), 4.46 - 5.38 (m, 4H, C1-OH, C3-OH, C4-OH, C6-OH), 5.62 (d, H, $^3J_{C1H-C2H}$ = 5.2 Hz, C1-H), 6.6 - 8.12 (6H, Ar-H), 8.9 (d, H, CH=N), 13.6 (t, H, Aromatic-OH). ESI MS m/z = 334 ($[M+H]^+$, 100 %). Anal. calcd. for $C_{17}H_{19}O_6N$; C, 61.25; H, 5.75; N, 4.20; Found; C, 61.34; H, 5.86; N, 4.28.

Synthesis of **C2**: To a suspension of anthracenaldehyde (0.33 g, 1.6 mmol) in ethanol (10 ml) *cyclohexylamine* was added (0.16 g, ~190 µl, 1.6 mmol). The reaction mixture was

allowed to reflux at 50 ºC for 24 hrs and was brought to room temperature. Yellow solid was formed which was separated by filtration and washed with small portions of ice cold ethanol. Yield (1.51 g, 58%) ^{1}H NMR (DMSO-d_6, ppm): δ 2.05 – 1.28 (m, 10H, Cyclohexane-Hs), 3.56 – 3.51 (H, p, $^{3}J_{C1H-C2H}$ = 6 Hz, C1-H), 7.25 – 7.51 (4H, C5 and C6 Hs of anthracene), 7.98 – 8.01 (2H, C4Hs of anthracene), 8.44 – 8.46 (3H, C1, C8 and C10 Hs of Anthracene), 9.42 (s, H, CH=N). ESI MS m/z = 288 ([M+H]$^{+}$, 100 %). Anal. calcd. for $C_{21}H_{21}N$; C, 87.76; H, 7.36; N, 4.87; Found; C, 87.84; H, 7.48; N, 4.81.

Synthesis of **C3**: To a suspension of anthracenaldehyde (2.06 g, 10 mmol) in ethanol (15 ml) *n*-butylamine was added (0.73g, ~1ml, 10 mmol). Yellow solid was formed instantly. The reaction mixture was allowed to reflux at 50ºC for 24 hrs and was brought to room temperature. The solid product was separated by filtration and washed with small portions of ice cold ethanol. Yield (1.51 g, 58%); IR (KBr): 2835, 2857, 2953 (S) $\upsilon_{(C-H)}$, 1642 (S) $\delta_{(CH=N)}$.cm^{-1}; ^{1}H NMR (DMSO-d_6): 1.047-1.084 (t, 3H, -CH_3), 1.534-1.627 (sextet, 2H, -CH_2-), 1.887-1.960 (q, 2H, -CH_2-), 3.937-3.972 (t, 2H, N-CH_2-Bu), 7.260 (S, $CHCl_3$), 7.468-8.479 (m, 6H, Ar-H), 9.405 (S, 1H, CH=N) ppm; ESI MS: m/z 261.15 ([M+H]$^{+}$, 100%); Anal. calcd. for $C_{19}H_{19}N$: C, 87.31; H, 7.33; N, 5.36 found C, 87.22; H, 7.39; N, 5.41.

Characterization of **L**

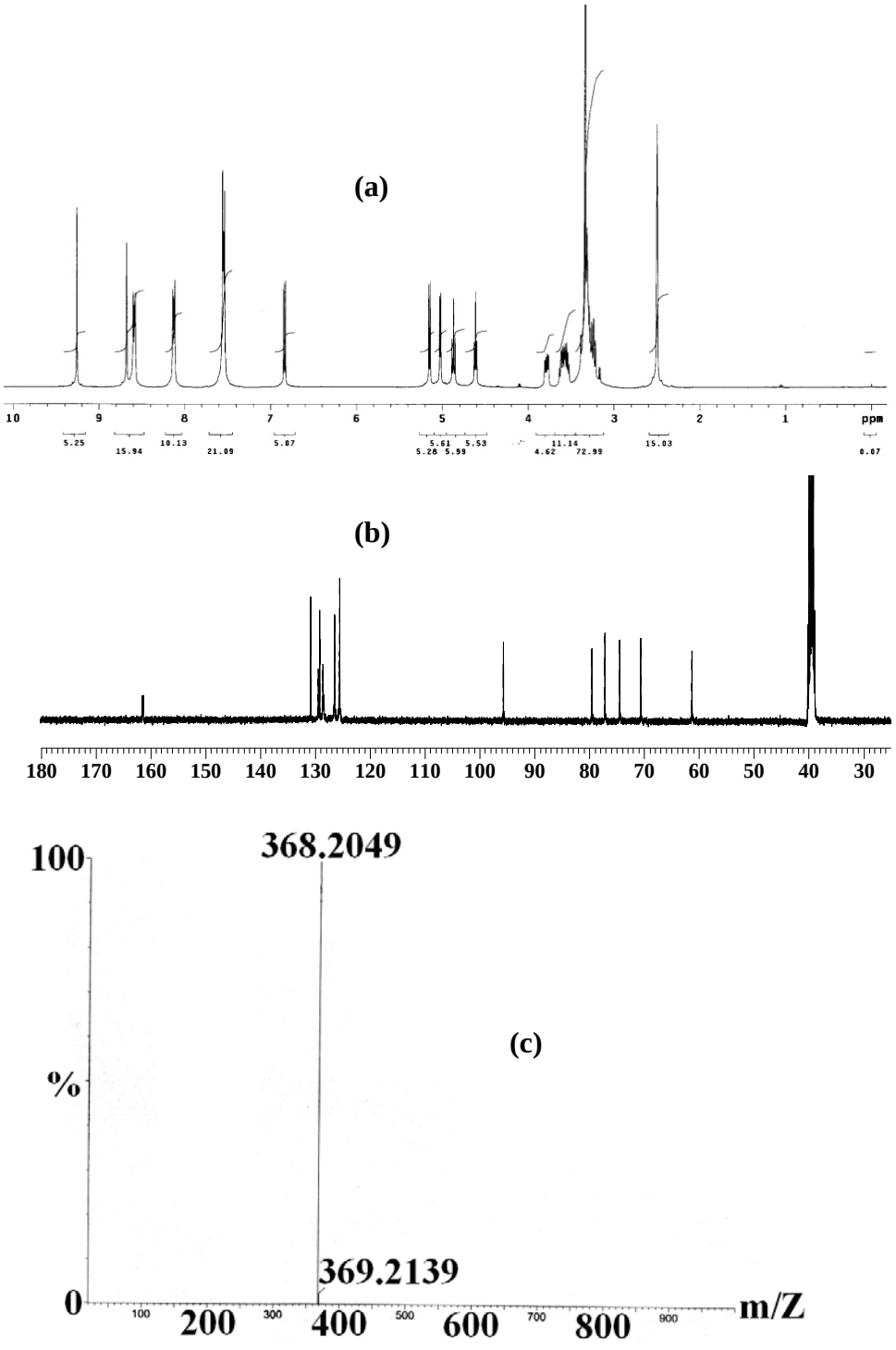

Figure 01: Spectral traces for **L**; (a) ^{1}H-NMR and (b) 13C-NMR and (c) ESI-MS spectral traces.

Characterization of **C1**

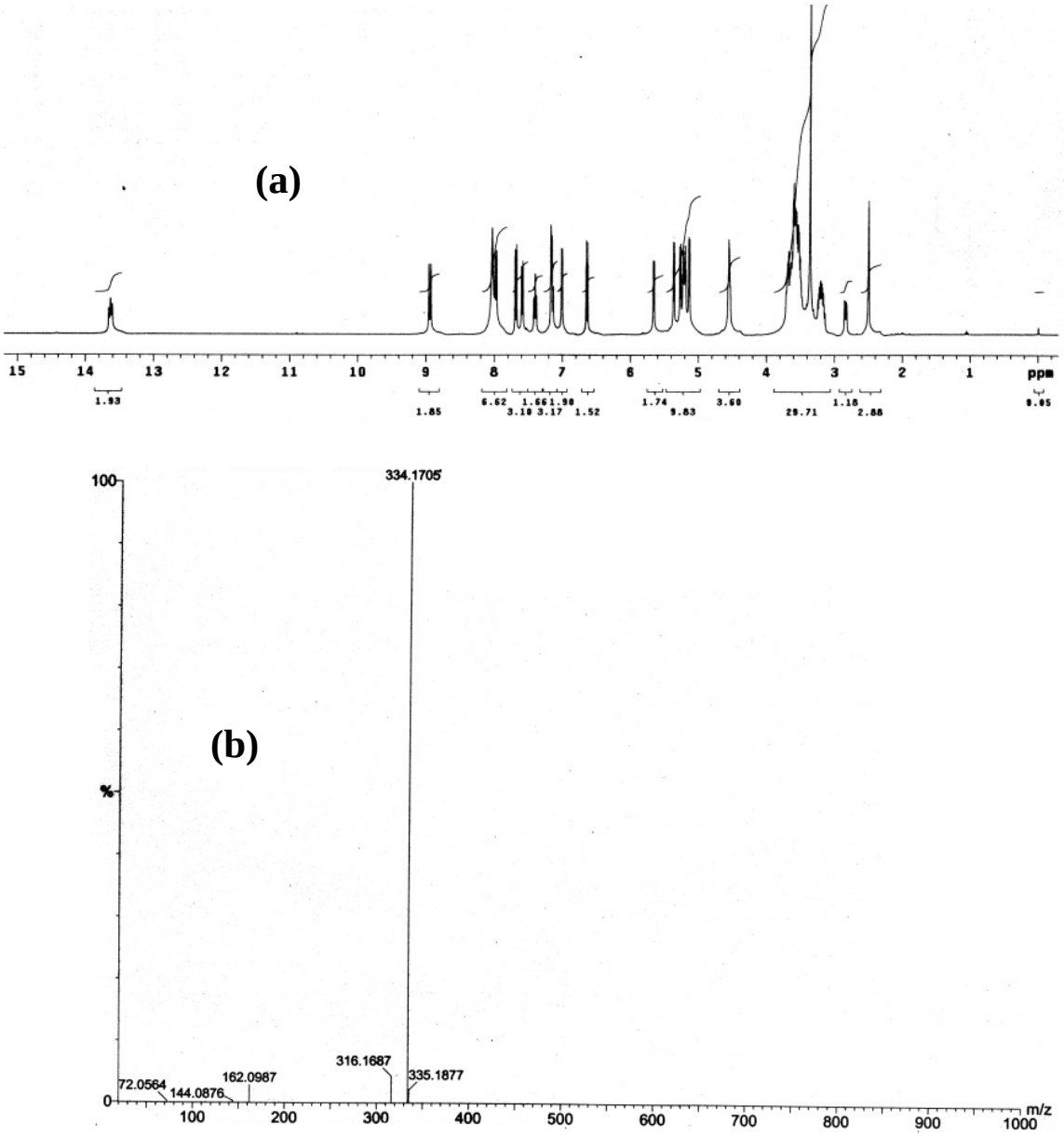

Figure 02: NMR spectra for **C1** as measured in DMSO-d_6: (a) ^{1}H, (b) ESI-Mass spectrum for **C1**.

Characterization of **C2**

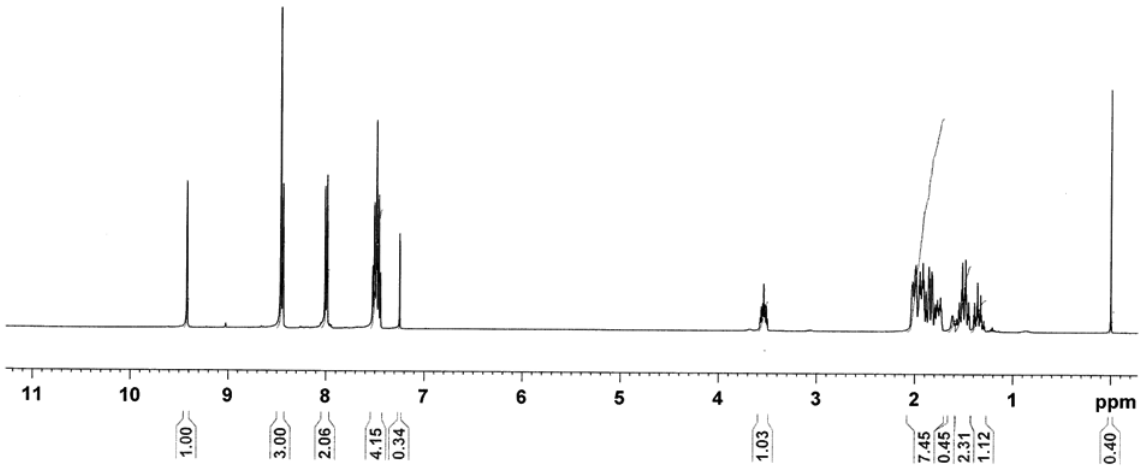

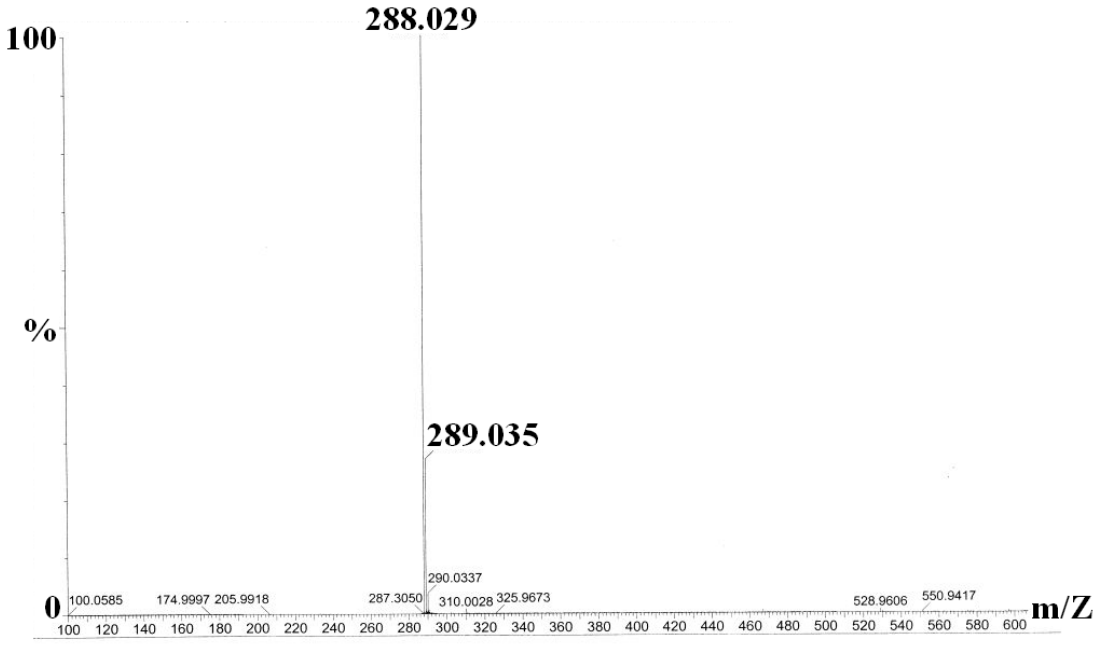

Figure 03: NMR spectra for **C2** as measured in $CDCl_3$: (a) ^1H, (b) ESI-Mass spectrum for **C2**.

Characterization of **C3**

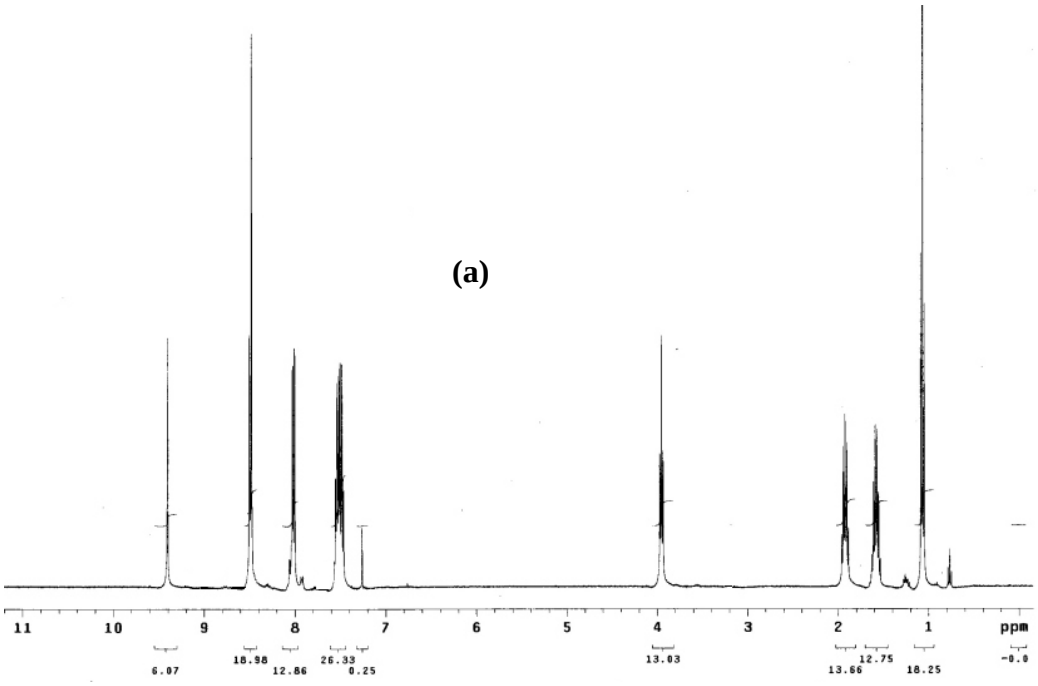

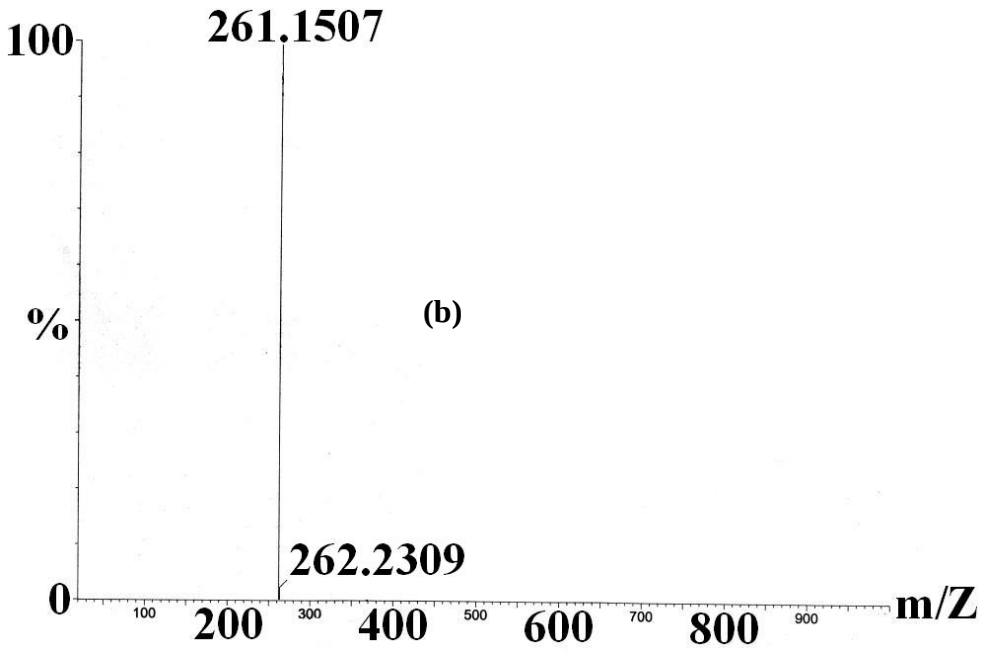

Figure 04: Characterization of **C3**; (a) ^{1}H-NMR and (b) ESI-MS for **C3**.

SI 02: Fluorescence titration of **L** against M^{n+}:

In order to carry out the fluorescence titrations, stock solution of 10^{-3} M of **L** and $\mathbf{L_1}$ were prepared by dissolving requisite amount of **L** in 100 μL of DMSO and $\mathbf{L_1}$ in 200 μL of $CHCl_3$ and then the volume was made up by aqueous methanol or ethanol. A stock solution of 10^{-3} M metal perchlorate was prepared in the same solutions. The requisite volume of the metal ion solution was added to a 50 μL **L** and $\mathbf{L_1}$ solution to get the corresponding ligand to metal ion mole ratio by making the total volume to 3 ml using aqueous CH_3OH/C_2H_5OH.

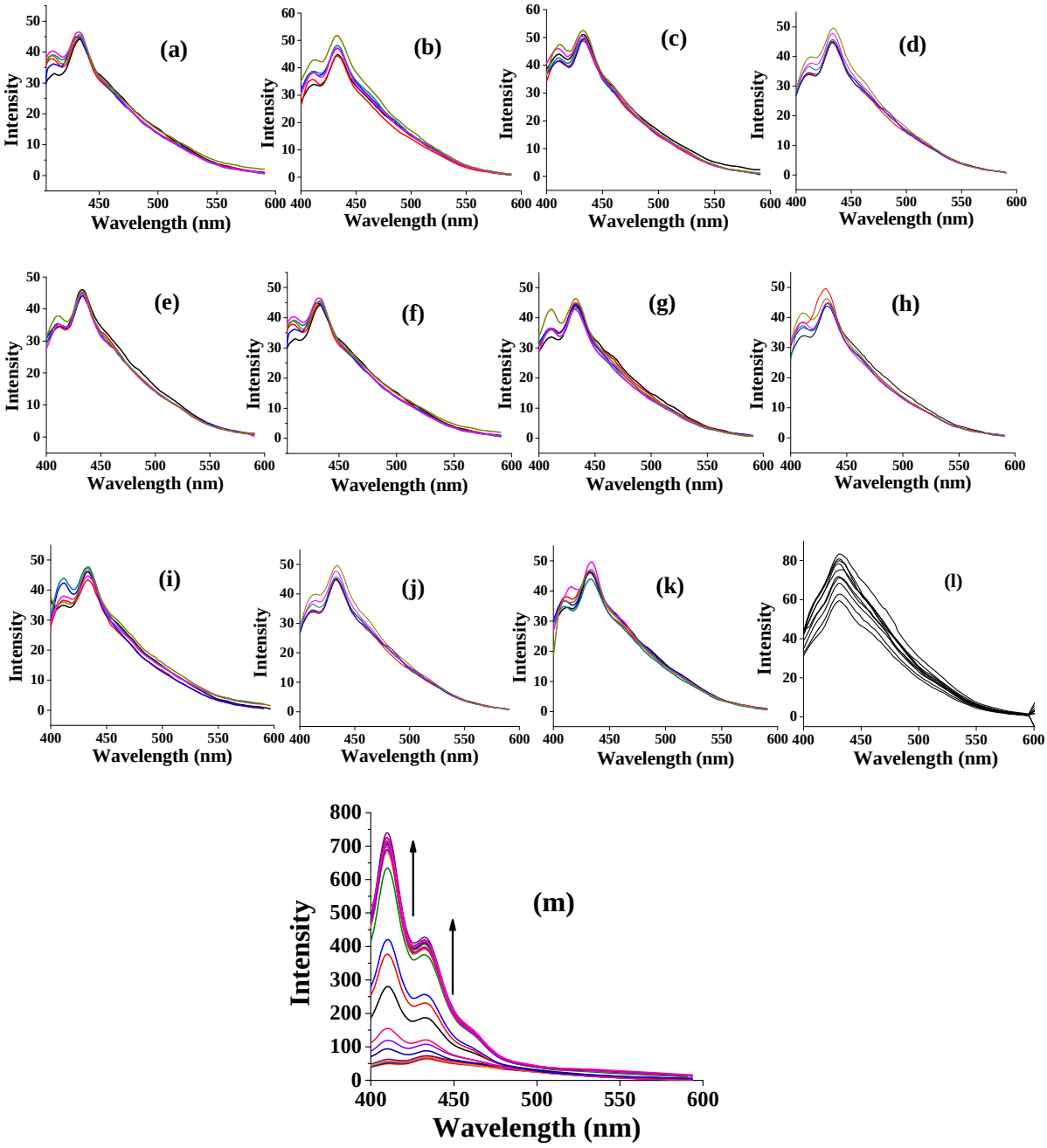

Figure 05: Fluorescence spectral traces for **L** against (a) Na^{+}, (b) K^{+}, (c) Ca^{2+}, (d) Mg^{2+}, (e) Mn^{2+}, (f) Fe^{2+}, (g) Co^{2+}, (h) Ni^{2+}, (i) Cu^{2+}, (j) Zn^{2+}, (k) Cd^{2+}, (l) Pb^{2+}, and (m) Hg^{2+}.

SI 03: UV-Vis titration between **L** and athracene against Hg^{2+} & Naked eye sensing of Hg^{2+} by **L**

For the absorption titrations, 2 x 10^{-3} M stock solutions of **L**, $\mathbf{L_1}$ and metal perchlorates were prepared and the solutions were made by following the procedure similar to that employed in case of fluorescence titrations. In case of Job's plot experiment, stock solution of 2 x 10^{-3} M of **L** and 1 x 10^{-3} M of metal perchlorates were prepared and a standard protocol was followed. The solutions made for absorption titrations were also used for the naked eye detection carried out by watching the color change.

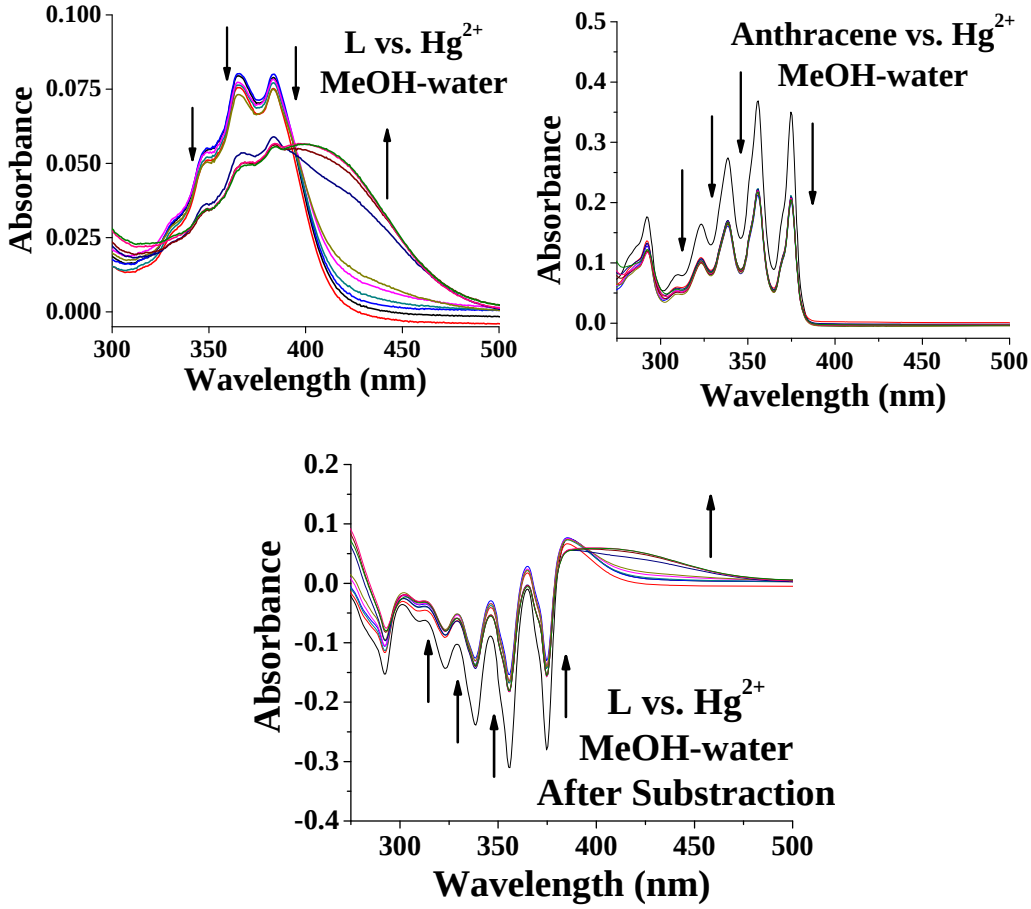

Figure 06: Absorption titration traces between (a) L *vs*. Hg^{2+}, (b) control molecule anthracene *vs*. Hg^{2+} and (c) subtracted spectra indicating the role of imine moiety in the Hg^{2+} binding.

Naked eye sensing of Hg^{2+} with **L**

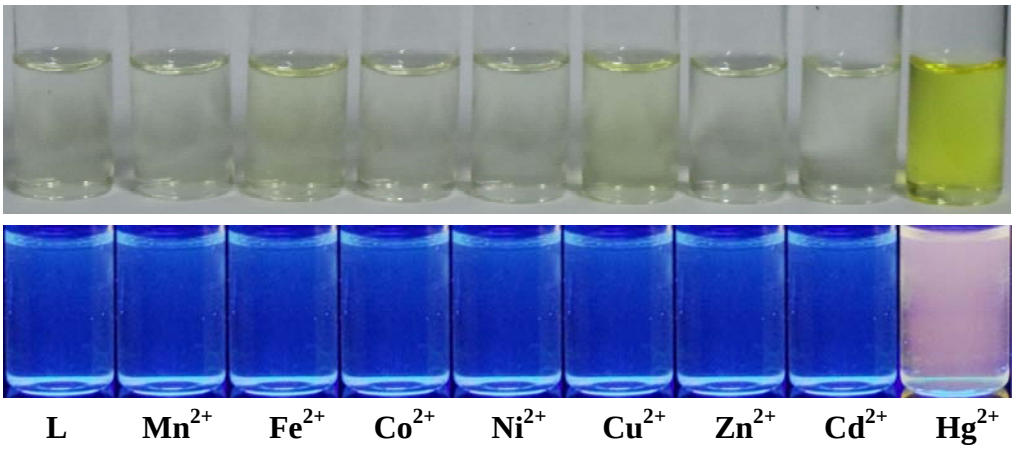

Figure 07: Naked eye sensing of Hg^{2+} under (a) visible and (b) UV light.

SI 04: Fluorescence and absorption titration against the control molecule **C1, C2** and **C3**

Fluoescence spectral traces:

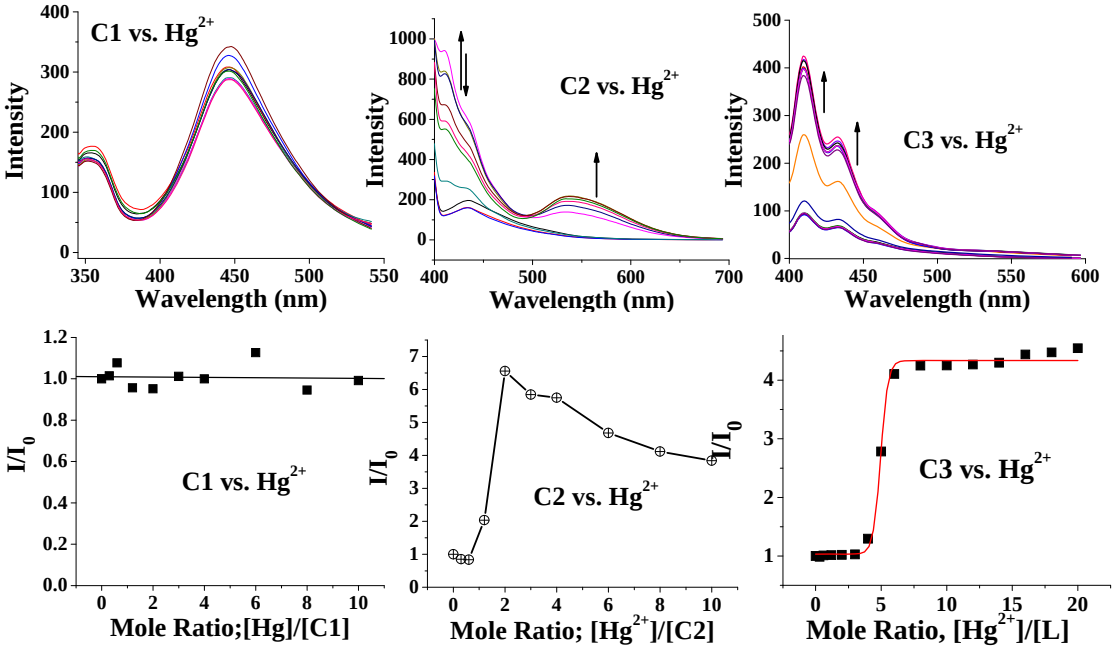

Absorption spectral traces:

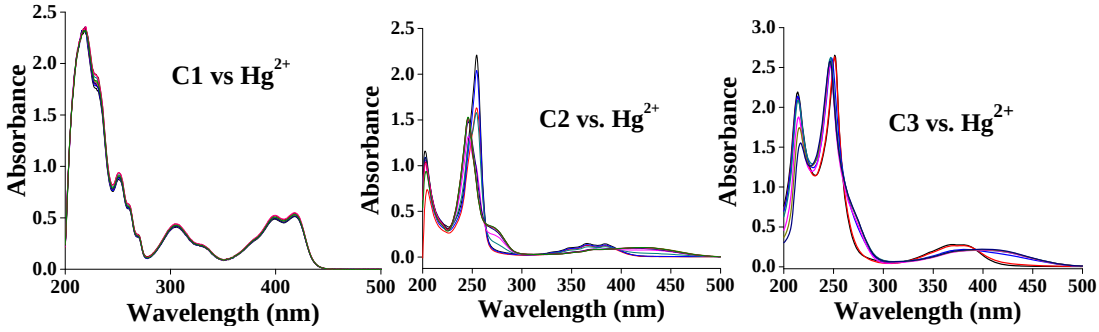

Figure 09: Fluorescence and absorption spectral traces for the titration of **C1, C2** and **C3** against Hg^{2+}.

SI 05: ^{1}H-NMR titration of **L** against Hg^{2+}.

^{1}H NMR titration of L with Hg^{2+}: **L** (0.0076 M) was dissolved in 0.4 mL of DMSO-d_6 and recorded the ^{1}H NMR spectra. Metal ion titrations were carried out by adding different volumes of, *viz.*, 20, 40, 80 and 160 μL of bulk $Hg(ClO_4)_2.6H_2O$ (0.076 M) solution to a solution of **L** to result in $[Hg^{2+}]/[\mathbf{L}]$ mole ratio of 0 - 4.

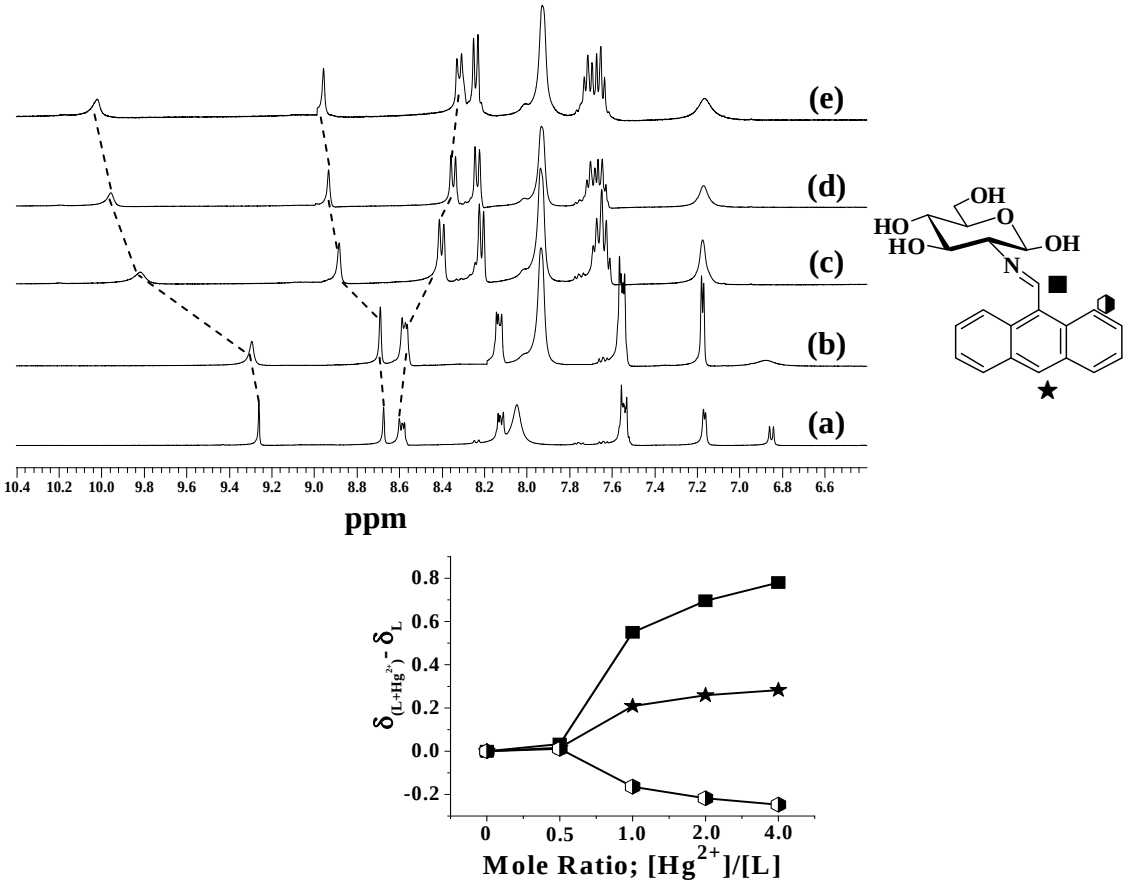

Figure 08: ^{1}H-NMR titration for **L** against $Hg(ClO_4)_2$ in DMSO-d6; 1H-NMR spectral traces for (a) **L** only, (b) **L** + 0.5eq. Hg^{2+}, (c) **L** + 1.0eq. Hg^{2+}, (d) **L** + 2.0eq. Hg^{2+} and (e) **L** + 4.0eq. Hg^{2+}. Change in the chemical shift value upon addition of Hg^{2+} to the solution of **L** using DMSO-d6 as solvent. Symbols ■, ★ and ◑ indicate the changes for imine, C10 and C1 protons of the receptor molecule.

SI 06: Fluorescence titration against proteins

Biological applicability of **L** to sense Hg^{2+} has been addressed by carrying out fluorescence titrations using human blood serum, milk medium as well as related albumin proteins, *e.g.*., human serum albumin (HSA), bovine serum albumin (BSA) and even milk protein (predominantly casein). Fluorescence experiments were carried out by taking an *in situ* generated $\{(\mathbf{L})_2Hg^{2+}\}$ complex and titrating this by varying the concentrations of blood serum, milk or the related proteins (HSA, BSA, Milk protein). Almost no change was observed in the fluorescence intensity of **L** at 410 nm band either in the presence of these proteins added individually or in the presence of the serum and milk. In case of the reverse titrations, the receptor system (**L**) was added with 10 equivalents of blood serum and milk medium or the proteins of interest (BSA, HSA and Milk protein). The resulting solution was then titrated against increasing amount of Hg^{2+}.

Protein titration against *in situ* [**L**-Hg^{2+}] complex

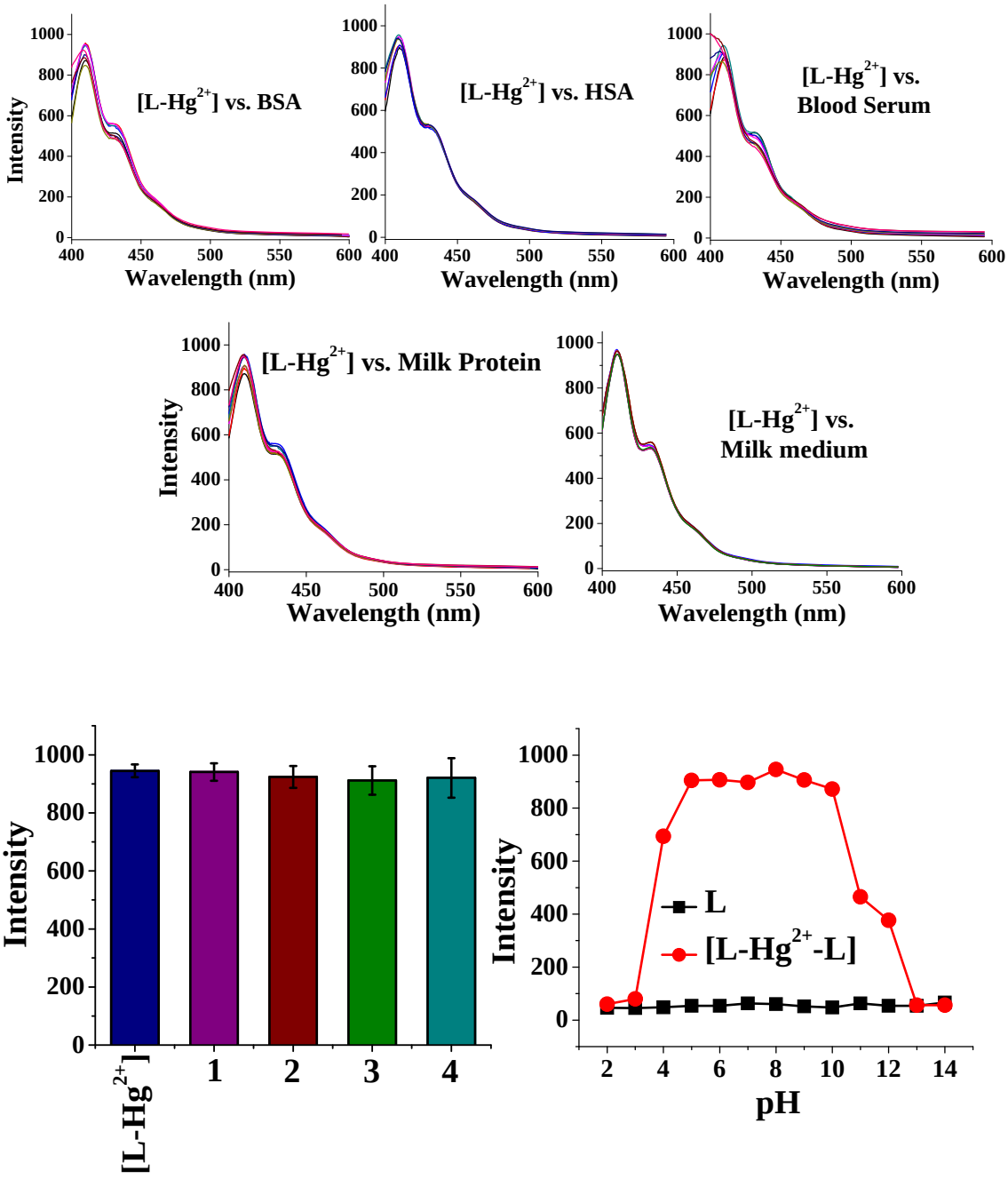

Figure 10: Fluorescence spectral traces for the titration of (a) BSA, (b) HSA, (c) human blood serum, (d) milk protein, and (e) milk medium against in situ prepared [**L**-Hg^{2+}] complex; (e) intensity observed during the titration of {**L** + X} against Hg^{2+} where **1** = BSA, **2** = HSA, **3** = Blood serum, **4** = milk protein, and (f) working pH range for the receptor system **L**.

Hg^{2+} titration of **L** in presence of proteins

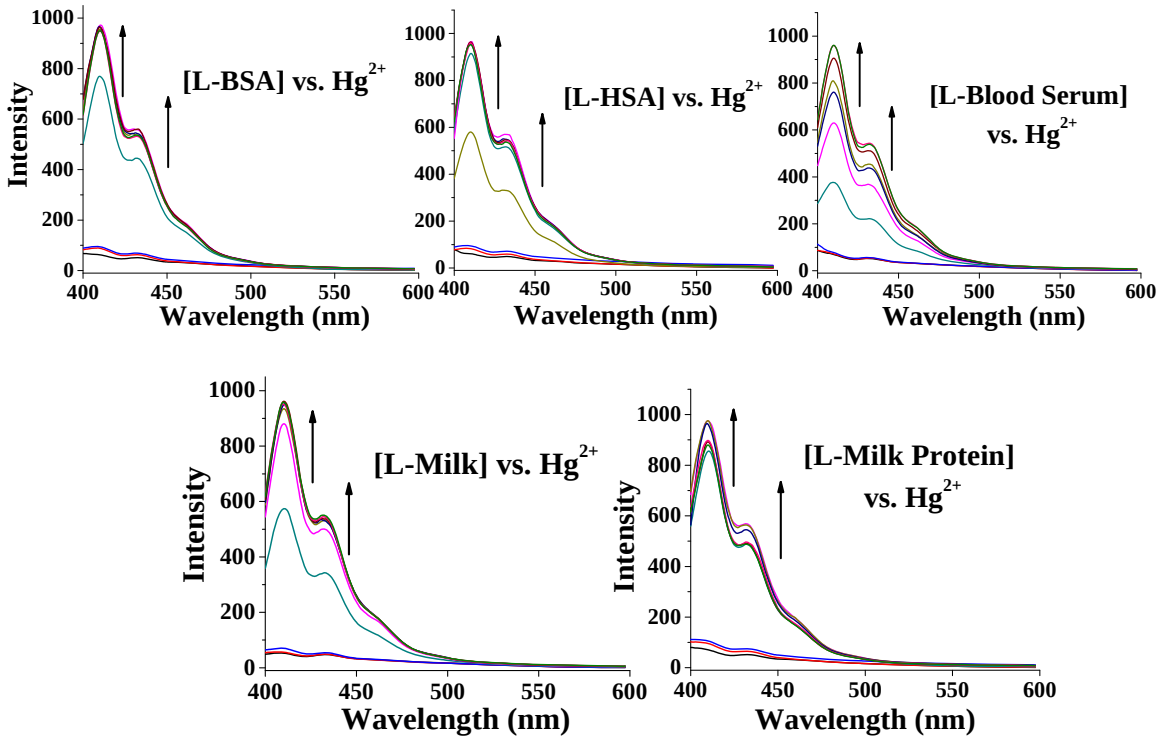

Figure 11: Fluorescence spectral traces for the titration of **L** against Hg^{2+} in presence of excess amount of (a) BSA, (b) HSA, (c) human blood serum, (d) milk medium, and (e) milk protein.

SI 07: Detection Limit for Hg^{2+} by **L** using fluorescence spectroscopy

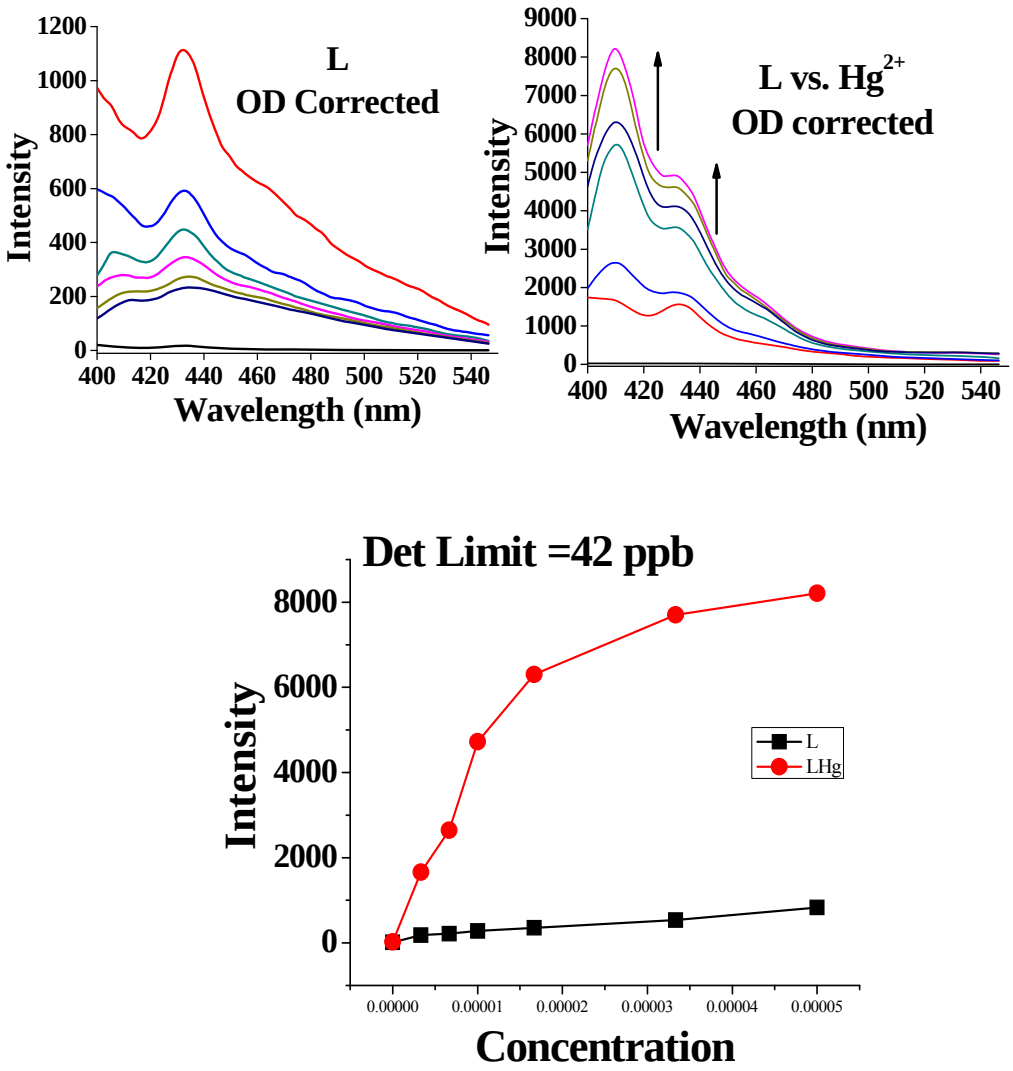

Figure 12: Fluorescence titration to find out the detection limit for Hg2+ using L is aqueous methanol.

SI 08: Fluorescence enhancement for **L** in presence of 2 ppb Hg^{2+}

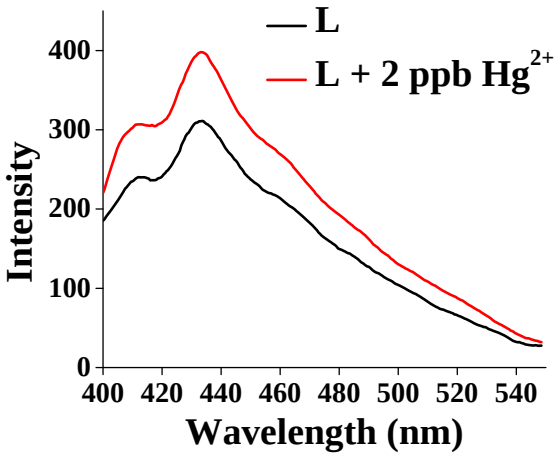

Figure 13: Fluorescence intensity of **L** and (**L** + 2 ppb Hg^{2+}) in aqueous methanol.

SI 09: **Computational Calculations**: In order to understand the interactions present between **L** and Hg^{2+}, computational studies were carried out in a systematic fashion by going through the sequence of computational levels, viz., semi empirical --→ *ab initio* --→ HF --→ DFT. As the formation of 2:1 species was already established by ESI-MS and supported by the Job's plot, the 2:1 species were optimized using Gaussian 03 package.[ref] Prior to assuming the initial guess model for computational calculations, **L** was independently optimized by using different theories as mentioned above by a cascade fashion up to DFT level of theory. The complex of **L** with Hg^{2+} was made by simply placing the metal ion far away from both the **L** in such a way that the imine-N atoms of these are pointed towards the Hg^{2+}. Then the complex was optimized in a cascade manner and finally using B3LYP/CEP-121G level of theory. The results obtained at this level were used in the discussion.

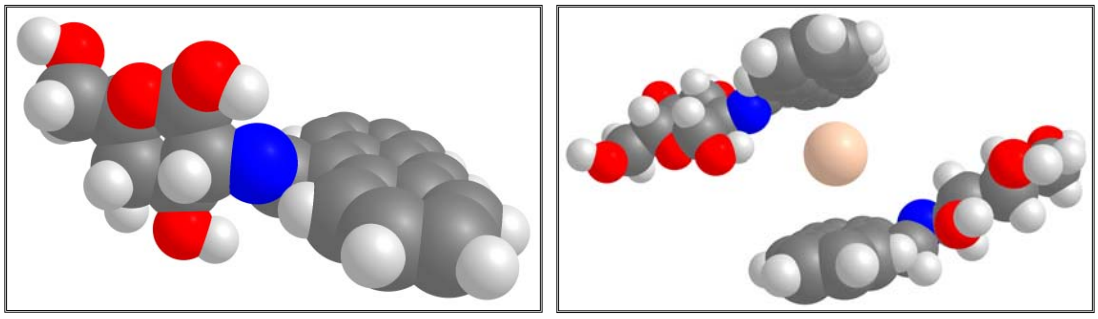

Figure 14: DFT optimized structure of (a) **L** and (b) **[L-Hg^{2+}-L]** complex.

Coordinates for the optimized [L-Hg^{2+}-L] complex

6	7.952436706	-1.513183567	-0.325321922
6	7.970466175	-0.442979483	0.799086648
6	6.895860099	0.650686564	0.555365406
6	5.522328404	0.004584742	0.292397334
6	5.673861730	-1.051273362	-0.834623040
1	7.757921021	-0.923821623	1.763020130
1	8.257783161	-1.044615045	-1.272892410
1	5.225939096	-0.554875742	1.189835586
1	6.028720662	-0.569381339	-1.762960345
1	7.209485784	1.236995990	-0.322051612
6	8.847371938	-2.722381699	-0.048811341
1	9.871768692	-2.388093905	0.145518263

1	8.466987790	-3.262559868	0.827014442
8	8.791624063	-3.627302490	-1.171742404
1	9.675408333	-3.714680949	-1.575996935
8	9.237619983	0.245169468	0.838694961
1	9.784070257	-0.075161790	1.582553359
8	6.783403608	1.511246824	1.704428364
1	7.650594590	1.944671991	1.844208008
8	6.605631152	-2.042267556	-0.436379614
8	4.453775168	-1.723910314	-1.082046291
1	3.756241772	-1.074817267	-0.853662284
7	4.366233880	0.834152545	-0.082156246
1	2.888131518	1.547898303	-4.565506679
6	2.430551413	2.104346273	-3.751106091
6	2.994794240	2.068392337	-2.495026281
6	1.263029884	2.886776316	-4.011142358
6	2.433956443	2.815410446	-1.397161014
1	3.884573688	1.476793868	-2.324484360
6	0.700419097	3.623395661	-2.996458459
1	0.846903930	2.915400110	-5.014769225
6	2.998810566	2.837536046	-0.086010237
6	1.266769553	3.618819296	-1.674412718
1	-0.173272566	4.244921180	-3.179245246
6	2.418540002	3.653169582	0.931591938
6	0.706509663	4.410220229	-0.658606805
6	2.926747452	3.700509591	2.278886310
6	1.254540128	4.448611895	0.632200918
1	-0.169318035	5.016399031	-0.881704756
6	2.341938861	4.499377600	3.235131085
1	3.782952135	3.094000668	2.555310631
6	0.669605514	5.268122175	1.657648206
6	1.199966433	5.300553923	2.924219433
1	2.749496460	4.525099570	4.242337709
1	-0.202137717	5.866991282	1.404149011
1	0.760506651	5.927958301	3.694398693
6	4.213906379	2.053311983	0.278448318
1	4.951920406	2.562423349	0.903681537
1	0.435926449	-4.726060068	0.993304520
6	-0.541240314	-4.265702466	0.869791218
6	-1.161041471	-3.663345630	1.991599281
6	-1.143610444	-4.264611430	-0.408717707
6	-0.519205053	-3.653241400	3.246231095
6	-2.470540849	-3.057203738	1.850704298
6	-2.438552034	-3.643707314	-0.580682495
6	-0.474624950	-4.806207416	-1.527917377
6	-1.137376685	-3.057329446	4.361283224

1	0.459160295	-4.112803862	3.354191002
6	-3.076814536	-2.494162912	2.991823558
6	-3.108933587	-3.072885296	0.562686636
6	-2.972161644	-3.546462607	-1.880635197
6	-1.043018479	-4.719161349	-2.809598233
1	0.495234963	-5.278772927	-1.398497638
6	-2.402591497	-2.485311641	4.232005950
1	-0.625659233	-3.054406027	5.319309436
1	-4.059934840	-2.044637207	2.928483858
6	-4.451380205	-2.489090369	0.357724356
6	-2.272734924	-4.081083030	-2.984627065
1	-3.906591108	-3.023549052	-2.058196505
1	-0.513704251	-5.133781453	-3.662673520
1	-2.891352602	-2.030064450	5.088945792
7	-4.693024011	-1.299036024	0.757596040
1	-5.171968861	-3.086775052	-0.210068188
1	-2.698394676	-3.981636631	-3.979574402
6	-5.988550343	-0.714601822	0.394094498
6	-5.885885309	-0.155073783	-1.044232384
6	-6.337931566	0.412619045	1.373834119
1	-6.801949434	-1.450813918	0.427776221
6	-7.127782595	0.670613642	-1.434711495
1	-5.016977583	0.516082880	-1.111099860
8	-5.677435582	-1.285943555	-1.907671033
1	-5.529473519	1.163291427	1.414434537
8	-7.552977508	1.030585084	0.960603525
8	-6.527404514	-0.174867663	2.645831943
6	-7.446384367	1.710267892	-0.326101971
1	-7.983732822	-0.005495976	-1.565713089
8	-6.776772652	1.314268321	-2.673867034
1	-5.917486488	-1.047141393	-2.831327123
1	-7.118599737	0.400512345	3.172639690
1	-6.631918911	2.448592451	-0.295569821
6	-8.762178957	2.454383586	-0.520517076
1	-7.552262956	1.396858284	-3.262536634
1	-8.891233436	2.708751357	-1.581506663
1	-9.590853072	1.807385238	-0.200917321
8	-8.690318289	3.648812235	0.278730745
1	-9.584013686	4.022671288	0.403192063
80	-0.225705361	0.176682822	-0.269864213

Total reference of Gaussian03: M. J. Frisch, G. W. Trucks, H. B. Schlegel, G. E. Scuseria, M. A. Robb, J. R. Cheeseman, Jr. J. A. Montgomery, T. Vreven, K. N. Kudin, J. C. Burant, J. M. Millam, S. S. Iyengar, J. Tomasi, V. Barone, B. Mennucci, M. Cossi, G. Scalmani, N. Rega, G. A. Petersson, H. Nakatsuji, M. Hada, M. Ehara, K. Toyota, R. Fukuda, J. Hasegawa, M. Ishida, T. Nakajima, Y. Honda, O. Kitao, H. Nakai, M. Klene, X. Li, J. E. Knox, H. P. Hratchian, J. B. Cross, C. Adamo, J. Jaramillo, R. Gomperts, R. E. Stratmann, O. Yazyev, A. J. Austin, R. Cammi, C. Pomelli, J. W. Ochterski, P. Y. Ayala, K. Morokuma, G. A. Voth, P. Salvador, J. J. Dannenberg, V. G. Zakrzewski, S. Dapprich, A. D. Daniels, M. C. Strain, O. Farkas, D. K. Malick, A. D. Rabuck, K. Raghavachari, J. B. Foresman, J. V. Ortiz, Q. Cui, A. G. Baboul, S. Clifford, J. Cioslowski, B. B. Stefanov, G. Liu, A. Liashenko, P. Piskorz, I. Komaromi, R. L. Martin, D. J. Fox, T. Keith, M. A. Al-Laham, C. Y. Peng, A. Nanayakkara, M. Challacombe, P. M. W. Gill, B. Johnson, W. Chen, M. W. Wong, C. Gonzalez, J. A. Pople, *Gaussian 03*, revision C.02; Gaussian, Inc.: Wallingford, CT, 2004.

SI 10: Proof of reversibility of Hg-binding by L; titration against 50 mM Na_2EDTA:

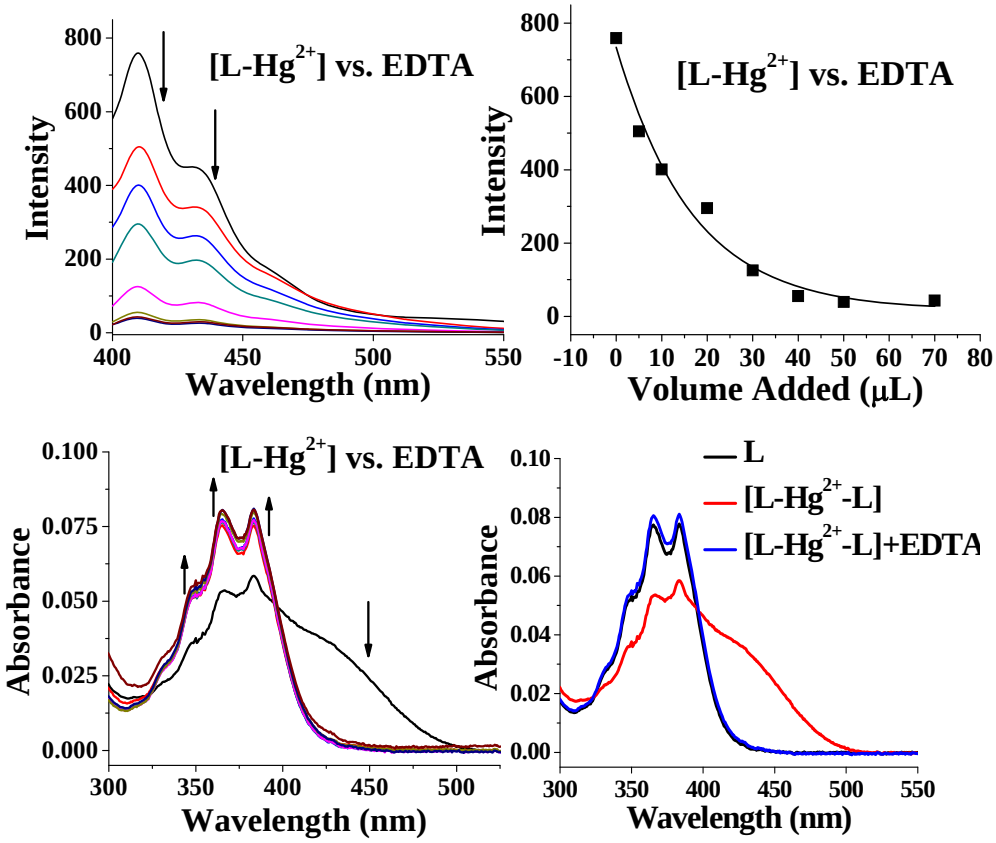

Figure 15: Reversibility in Hg^{2+} binding by **L**; (a) fluorescence quenching of *in situ* [**L**-Hg^{2+}-**L**] complex up on addition of increasing volume of 50 mM Na_2EDTA solution, (b) Intesity vs. volume of EDTA plot, (c) absorbance titration of *in situ* [**L**-Hg^{2+}-**L**] complex against 50 mM EDTA solution, and (d) absorption spectral traces for **L**, [**L**-Hg^{2+}-**L**], and {[**L**-Hg^{2+}-**L**] + 10 μL EDTA} showing the displacement of Hg^{2+}.